Catalysis Today 151 (2010) 202–211

Contents lists available at ScienceDirect

Catalysis Today

journal homepage: www.elsevier.com/locate/cattod

Diesel NO_x aftertreatment catalytic technologies: Analogies in LNT and SCR catalytic chemistry

Pio Forzatti, Luca Lietti, Isabella Nova*, Enrico Tronconi

Dipartimento di Energia, Laboratory of Catalysis and Catalytic Processes, Politecnico di Milano, p.za Leonardo da Vinci, 32, 20133 Milano, Italy

ARTICLE INFO

Article history:
Available online 29 March 2010

Keywords:
Diesel aftertreatment technologies
Lean NO_x Trap
SCR
Nitrites
Nitrates
Ammonia

ABSTRACT

This paper reviews the main results of wide investigations dedicated to the understanding of the chemistry and the reaction pathways operating in the reduction of NO_x in LNT and SCR processes for the aftertreatment of NO_x in diesel exhausts. In particular, similarities and differences between the two processes will be highlighted.

The reactions involved in the NH_3-NO/NO_2-SCR reacting system were investigated by an extensive set of various unsteady-state experiments performed over both vanadium-based and zeolite-based commercial catalysts: the bulk of results led to the proposal of an original global mechanistic scheme of the complete NH_3-NO/NO_2-SCR reacting system. In such a scheme, a key role is played by nitrite and nitrate species, which are formed by NO_2 disproportion onto catalyst surfaces. Nitrites are readily reduced by ammonia to dinitrogen, whereas the rate limiting step is the reduction of surface nitrates, performed both by NO at lower temperatures and by NH_3 at higher temperatures possibly via formation of nitrites as intermediates in both cases.

The systematic study of LNT processes showed that during the lean phase NO_x is stored onto the catalyst in the form of nitrite and nitrate species. It was also shown that during the subsequent reduction phase NO_x ad-species are reduced to dinitrogen through two consecutive steps in which NH_3 is formed as an intermediate upon reaction of nitrates with H_2, and further reacts with nitrates to selectively produce N_2.

Accordingly, in both LNT and SCR chemistries the reduction of NO_x involves nitrite and nitrate surface species, which are selectively reduced to nitrogen by ammonia, either formed as an intermediate or supplied as a reactant.

1. Introduction

It is widely recognised that diesel engine vehicles are fated to significantly increase their worldwide market penetration, even in countries like the United States where the present market share is not as significant as that of gasoline engines. This is mainly due to the fact that diesel engines are inherently more thermodynamically efficient than gasoline engines and thus they offer the prospect of reducing emissions of carbon dioxide as well [1,2].

However, diesel cars produce higher emissions of nitrogen oxides (NO_x) and particulate matter (PM). The tail-pipe emission levels that can be achieved depend upon both the engine-out emissions and the performance of the emissions control system. Improvements in combustion and/or alternative fuels can lead to lower NO_x emissions, but it is widely accepted that in order to meet future legislative emissions standards (Euro 6 for light-duty vehicles and Euro VI for heavy-duty engines, as well as the US 2010 Bin5), the employment of after treatment systems will be required [1,2]. Indeed, diesel particulate filters (DPFs) will be needed to achieve the PM emission levels regardless of the system used to reduce NO_x. But, most importantly, the significant CO_2 reduction (i.e. the improved fuel consumption) that will also be dictated by future regulations, will imply a drastic decrease in the average temperature profile of the exhaust gases; in such conditions, the catalytic removal of NO_x is extremely challenging. In fact, a significant portion of the new test cycles (both the NEDC, New European Driving Cycle, and the WHTC, World Harmonized Transient Cycle), is characterized by very low exhaust temperature profile [2].

Currently, there are two main aftertreatment technologies under consideration as potentially compliant with such strict limits: the Lean NO_x Trap technique, which is used with direct injection gasoline and small diesel engines, and NH_3/urea Selective Catalytic Reduction (SCR) for larger diesel engines.

Lean NO_x Traps were first developed and put into the market by Toyota to remove NO_x from vehicles equipped with lean burn engines [3,4]. These systems work under cyclic conditions, alternating long lean phase during which NO_x is stored in the form of nitrites and nitrates, with a short rich excursion during which the stored NO_x is reduced to nitrogen (and other byproducts). LNT materials typically consist of a NO_x storage component, such as

* Corresponding author. Tel.: +39 0223993228; fax: +39 0223993318.
E-mail address: isabella.nova@polimi.it (I. Nova).

0920-5861/$ – see front matter © 2010 Elsevier B.V. All rights reserved.
doi:10.1016/j.cattod.2010.02.025

an alkaline earth metal oxide (e.g. Ba), and a noble metal (e.g. Pt) that catalyzes the oxidation of NO_x, CO and of hydrocarbons and the reduction of stored NO_x as well. In spite of the fact that these catalysts are being used at the commercial scale, common agreement on the mechanisms of the storage of NO_x [3–38] and of their subsequent reduction [3,4,39–66] is still lacking.

In contrast to LNTs, SCR systems are designed to catalytically reduce NO_x emissions in the oxygen rich environment of diesel exhaust by injecting urea as a reducing agent [67,68]. SCR is the European motor industry's main technology of choice to meet Euro IV and Euro V emissions requirements for heavy-duty diesel engines, and during the last year it has been announced by some manufacturers for light-duty applications in the US and more recently in Europe, as well [1]. A Diesel Oxidation Catalyst (DOC) is also usually present in the system configuration, upstream of the SCR converter, to partially convert NO to NO_2; this permits the flow entering the SCR reactor to contain significant amounts of NO_2 in addition to NO, and thus the onset of the SCR deNO_x reactions (the so-called Fast SCR reaction) can occur at lower temperature, in comparison to the case where most of NO_x is made of NO alone (standard SCR). However, only recently the study of the mechanisms active over conventional vanadium-based catalysts and over the new zeolite-based systems, when also significant amounts of NO_2 are present in the flue gases entering the SCR reactor, has been widely addressed in the literature [67–103].

During the last few years, both LNT and NO_2-related NH_3-SCR catalytic processes have been investigated in details in our labs [32–38,60–66,93–103]: this paper will report on the main results of these studies and in particular it will analyze the chemistry and the reaction pathways operating for the reduction of NO_x in both processes, in order to highlight analogies and differences between these two techniques.

2. Experimental

LNT – Homemade Pt–Ba/γ-Al_2O_3 (1/20/100, w/w) and Ba/γ-Al_2O_3 (20/100, w/w) model catalyst samples have been considered in the study. At first, a Pt/γ-Al_2O_3 sample was prepared by impregnation of γ-Al_2O_3 calcined at 700 °C (Versal 250 from UOP) with a solution of $Pt(NH_3)_2(NO_2)_2$ (Strem Chemicals, 5% Pt in ammonium hydroxide) followed by drying at 80 °C and calcination at 500 °C for 5 h. The obtained sample (S_a = 190 m^2/g; Pt dispersion = 82%) was impregnated with an aqueous solution of $Ba(CH_3COO)_2$ (Strem Chemical, 99%) and further calcined at 500 °C for 5 h to prepare the ternary Pt–Ba/γ-Al_2O_3 catalyst (S_a = 137 m^2/g; Pt dispersion = 70%). The Ba/γ-Al_2O_3 sample was prepared by impregnation of the bare γ-alumina support with barium acetate (S_a = 140 m^2/g). Further details on the preparation and characterisation of the samples are reported elsewhere [32–34].

Before catalyst testing, the samples were typically conditioned by performing a few adsorption/regeneration cycles with NO/O_2 (1000 ppm NO in He + 3%, v/v O_2) and H_2 (2000 ppm in He) at 350 °C, respectively, with an inert purge (He) in between. Conditioning lasted until a reproducible behaviour was obtained; generally, this required 3–4 cycles.

The adsorption of NO_x was performed by imposing a rectangular step feed of NO (1000 ppm in He + 3%, v/v O_2) or NO_2 (1000 ppm in He), followed by a He purge at the same temperature to promote the desorption of weakly adsorbed species. NO_x adsorption was carried out at different temperatures in the range 200–400 °C over the Pt–Ba/γ-Al_2O_3 catalyst and over the corresponding binary samples as well [32–36,38].

The reduction of NO_x adsorbed species was investigated by different procedures: (i) Isothermal Step Concentration (ISC) experiments, in which NO_x stored at different temperatures was removed by imposing step feed of different reducing agents (2000 ppm of H_2, 1000 ppm of ammonia or 2000 ppm of CO in He) at constant temperatures; (ii) Temperature Programmed Surface Reaction (TPSR) experiments, in which, after NO_x adsorption at different temperatures, the catalyst was cooled down to RT in flowing He and then heated at 10 °C/min under flow of H_2 or ammonia or CO up to 400 °C; (iii) Temperature Programmed Reaction (TPR) experiments, in which a flow of NO (1000 ppm) and reducing agent (hydrogen, ammonia or CO) was admitted to the reactor at room temperature and then the catalysts were linearly heated up to 500 °C at 10 °C/min. All experiments were also performed in the presence of 1% (v/v) H_2O in the stream [60–66]. Due to the dilute conditions used in these studies, experiments have been carried out under nearly isothermal conditions, i.e. in the absence of significant temperature effects during the runs.

The experiments were performed by loading 60 mg of catalyst (100–150 μm) in a quartz microreactor (6 mm, i.d.) and using a total flow rate of 100 cm^3/min (measured at 0 °C and 1 atm). The reaction temperature was measured and controlled by a thermocouple immersed in the catalyst bed. The reactor outlet was connected to a mass spectrometer for the complete analysis of reactants and products. Further details on the experimental apparatus and procedures can be found elsewhere [32,34,60,64].

SCR – The commercial catalyst used in this work was originally supplied in the form of a cordierite honeycomb monolith washcoated with an Fe-zeolite. For testing, the catalyst was crushed and sieved to 140–200 mesh to avoid mass transfer limitations. The catalyst powder (80 mg) was loaded in a flow-microreactor identical to that used in the case of LNT experiments. Gas mixtures fed to the reactor included NH_3, NO and NO_2 in different proportions, as well as H_2O (1%, v/v), O_2 (0–2%) and He as the carrier gas, with a total flow rate of 71 cm^3/min (measured at 0 °C and 1 atm). Gases exiting the reactor were continuously analyzed by two instruments in a parallel arrangement: a UV analyzer (ABB Limas 11 HV), which detects NH_3, NO and NO_2, and a mass spectrometer (Balzer QMS 200), which measures N_2, O_2, H_2O, NH_3, NO, NO_2 and N_2O concentrations. More details on the experimental setup are available elsewhere [96,98,101,102].

Before each test, the catalyst sample was conditioned for 3 h at 600 °C in a stream containing oxygen (2%, v/v) and water (10%, v/v) to obtain stable activity. Different kinds of transient runs are presented in this work, Isothermal Step Concentration (ISC), Temperature Programmed Surface Reaction (TPSR) and Temperature Programmed Reaction (TPR). In a typical ISC run, the reactor was kept at constant temperature under a flow of He + 1% H_2O, and step changes of feed NH_3, or NO or NO_2 concentrations were imposed. At the end, a temperature programmed desorption ramp (10 °C/min, T_{end} = 550 °C) in an inert atmosphere was typically run to clean up the catalyst surface.

TPSR runs included a preliminary phase in which NO_2 was fed and adsorbed onto the catalyst at constant temperature: subsequently a temperature programmed ramp (20 °C/min) was performed in the presence of gaseous NH_3 in the feed stream; these runs were performed to study the reactions between NH_3 and the surface species resulting from NO_2 adsorption.

Finally, in TPR runs different reactants were continuously fed to the reactor while the temperature was linearly heated from RT up to 500 °C at 10 °C/min.

3. Results and discussion

3.1. NO_x adsorption processes

LNT – In order to achieve a complete qualitative and quantitative understanding of the mechanism that governs the NO_x adsorption

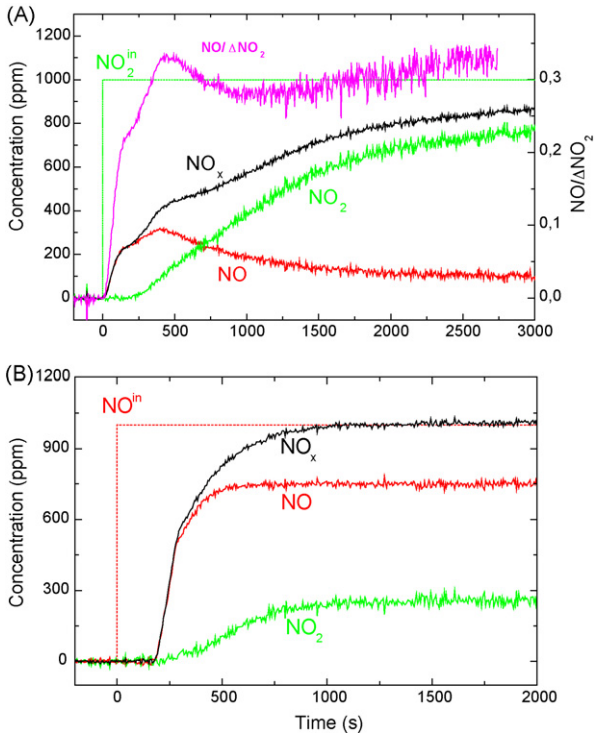

Fig. 1. (A) NO_2 (1000 ppm) adsorption at 350 °C over Ba/γ-Al_2O_3 catalyst. (B) NO/O_2 (1000 ppm/3%, v/v) adsorption at 350 °C over Pt–Ba/γ-Al_2O_3 (adapted from [34]).

phase, an extensive and systematic study was carried out in our labs over model Al_2O_3-supported Pt–Ba, Ba and Pt catalyst samples. Both FTIR spectroscopy and Isothermal Step Concentration (ISC) experiments were used as complementary techniques to collect information on the different surface and gaseous species formed upon interaction of NO, NO_2 and NO/O_2 mixtures [33–35].

Fig. 1A shows the adsorption of NO_2 at 350 °C over the binary Ba/γ-Al_2O_3 sample. Upon NO_2 admission to the reactor ($t = 0$ s) the NO_2 concentration trace exhibited a dead time of 200 s and then slowly increased reaching a final value near 800 ppm at t = 3000 s. The NO_2 adsorption is accompanied by NO evolution; the NO outlet concentration profile immediately increased upon NO_2 admission, showed a maximum of 300 ppm after roughly 400 s and then slowly decreased to a value near 100 ppm after 3000 s. At this time the storage was not yet complete, as the NO_x outlet concentration did not reach the inlet value; the amounts of NO_x adsorbed at the end of the run were estimated to be near 9×10^{-4} mol/g_{cat}.

Thus, the data showed that NO_2 adsorption is accompanied by NO evolution; at the end of the adsorption phase the overall amounts of adsorbed NO_2 and evolved NO roughly obeys the stoichiometry of the following disproportionation reaction:

$$3NO_2 + O^{2-} \leftrightarrow 2NO_3^- + NO \quad (1)$$

which implies the release of one NO molecule for every 3 NO_2 adsorbed molecules.

According to literature indications [3], reaction (1) results from two consecutive steps, reactions (2) and (3), in which at first NO_2 diproportionates to form simultaneously nitrites and nitrates, and then nitrites are very quickly oxidized to nitrates by further reacting with gaseous NO_2:

$$2NO_2 + O^{2-} \rightarrow NO_3^- + NO_2^- \quad (2)$$

$$NO_2 + NO_2^- \leftrightarrow NO_3^- + NO \quad (3)$$

so that only nitrates are present at the end of the run and the overall ratio between consumed NO_2 and evolved NO of reaction (1), is respected. Occurrence of reactions (2) and (3) accounts for the fact that the ratio between the evolved NO and the consumed NO_2 is initially lower than that expected according to the stoichiometry of reaction (1).

Similar results (not reported for brevity) were obtained over a Pt–Ba/γ-Al_2O_3 sample, but in this case the NO outlet concentration by far exceeded that expected from the occurrence of reaction (1), due to the NO_2 decomposition reaction catalyzed by Pt (reaction (4)):

$$NO_2 \leftrightarrow NO + 1/2O_2 \quad (4)$$

Notably, IR spectra showed on both the Ba/γ-Al_2O_3 and the Pt–Ba/γ-Al_2O_3 samples the formation of nitrates species only, already from the very beginning of the experiments [34,35]. As reported elsewhere [34,35], these nitrates were mainly of ionic type (bands at 1320, 1420–40 cm^{-1}, $\nu_{asym}NO_3$ split for the partial removal of the degeneracy; 1035–20 cm^{-1}, $\nu_{sym}NO_3$) and in minor amounts bidentate (1560 cm^{-1}, $\nu_{asym}NO_2$ mode expected around 1300 cm^{-1} obscured by the modes of ionic nitrates).

The adsorption process was also investigated starting from NO/O_2 mixtures over both the Ba/γ-Al_2O_3 and the Pt–Ba/γ-Al_2O_3 samples at 350 °C. In the case of the Ba/γ-Al_2O_3 sample (results not shown here) small amounts of NO_x species were adsorbed [34]. The FTIR spectra recorded at 350 °C showed a progressive formation of ionic nitrites (1220 cm^{-1}) on increasing the exposure time up to 10 min, along with small amounts of bridging nitrates. At higher exposure times, the band due to nitrite species decreased in intensity and completely disappeared after 20 min. In parallel, bands characteristic of ionic nitrate (1420, 1320, 1030 cm^{-1}) and in minor amounts of bidentate nitrates developed, so that after 20 min of exposure only nitrates were evident in the spectra.

The results collected feeding NO/O_2 mixture at 350 °C over the Pt–Ba/γ-Al_2O_3 catalyst are shown in Fig. 1B. At $t = 0$ s 1000 ppm of NO was added to the O_2/He feed flowing into the reactor: the concentration of NO showed a dead time, and then slowly increased with time up to its steady-state value. The evolution of NO_2 was also observed, after that of NO, due to the NO oxidation reaction (reverse reaction (4)). It was estimated that the catalyst was able to adsorb large amounts of NO_x (4.6×10^{-4} mol/g_{cat} at the end of the run).

The results of the corresponding FTIR analysis showed the immediate formation of nitrites upon NO admission in the presence of O_2 [34]; the bands of nitrite ad-species reached their maximum intensity after 1 min of contact. After 3–5 min of contact time only ionic nitrate species (and in minor amounts bidentate species) were evident on the catalyst surface. Notably, the rate of both nitrite formation and their oxidation to nitrates was higher over the Pt–Ba/γ-Al_2O_3 catalyst with respect to the binary Ba/γ-Al_2O_3 catalyst, pointing out a catalytic role of Pt.

Literature reports dealing with formation of NO_x adsorbed species over Pt–Ba/γ-Al_2O_3 catalysts are abundant [3–5,7–9,15,16,18,19,25,26,29,30], and a general consensus on the attribution of various IR bands related to the different species has been achieved. Nevertheless, open issues still remain: for instance, some authors proposed that ionic nitrates are actually bulk nitrates while bidentate nitrates are surface nitrates [29,30].

DRIFT data were also performed feeding NO/O_2 at 350 °C over the same Pt–Ba/γ-Al_2O_3 catalyst, under *operando* conditions equal to those used in the ISC experiments [35]. The results indicated that during the initial NO_x uptake, nitrites were more abundant than nitrates: the nitrite band intensity showed a broad maximum and then decreased with time on stream, while the nitrate bands presented a monotonous increase during the entire storage phase, so that at the end of the experiment (at 700 s ca.) nitrates were the prevalent adsorbed species. Thus, in line with FTIR data, in the adsorption process nitrites were intermediate species which then evolved leading to the formation of nitrates.

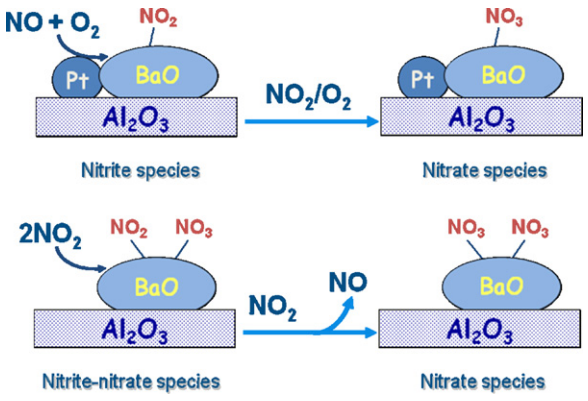

Fig. 2. Reaction pathway for NO_x adsorption over Pt–Ba/γ-Al_2O_3 catalysts.

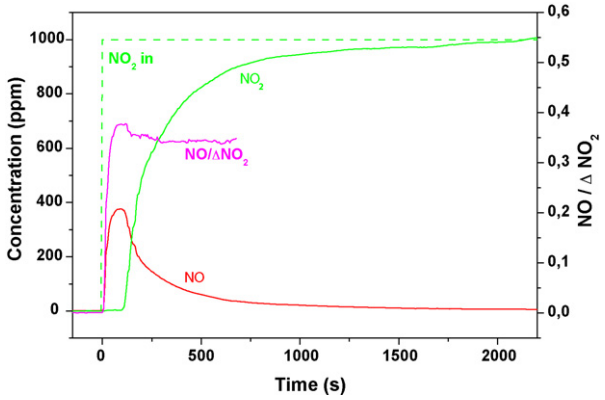

Fig. 3. NO_2 adsorption over Fe-zeolite. Feed flow = 71 cm^3/min (STP), NO_2 = 1000 ppm, NO = 1000 ppm, H_2O = 1% (v/v) in He at 150 °C (adapted from [102]).

On the basis of the previous and other results collected analyzing the adsorption process over Pt–Ba/γ-Al_2O_3 catalysts, the reaction pathway depicted in Fig. 2 was suggested for NO adsorption in the presence of oxygen.

In this scheme, NO_2 formed by NO oxidation over Pt sites easily adsorbs onto the Ba component of the catalysts through a disproportionation route with formation of nitrate and nitrite ad-species. Eventually nitrite ad-species are readily oxidized to nitrates by NO_2, so that at the end of adsorption only nitrate species are present on the catalyst surface. This pathway, that implies the direct adsorption of gaseous NO_2 on the Ba component, was referred to as the "nitrate route".

A different pathway was also suggested [34,38], which involves the direct uptake of NO in the presence of oxygen to form nitrites. This route does not imply the intermediate formation of gaseous NO_2, and is herein referred to as the "nitrite route". The nitrites formed in this way are then progressively oxidized by NO_2 (and/or O_2) to nitrates, which then are the prevailing species at catalyst saturation in the experiments performed with both NO_2 or NO/O_2 mixtures. It was suggested that the "nitrite route" implies a stepwise oxidation of NO to nitrites involving Ba species neighbouring to Pt sites or Pt–Ba couples [34,38]. Indeed, dedicated experiments in which the effect of the Ba loading (up to 30% by weight) in ternary Pt–Ba(x)/γ-Al_2O_3 catalysts [36] was considered, both the NO_x breakthrough time and the storage capacity of the catalysts increased with the Ba content up to a maximum observed for the catalyst sample having a Ba loading of 23% (w/w). Moreover the increase in the Ba loading resulted in a strong increase of the fraction of Ba involved in the storage, i.e. from 4% of the loaded Ba for the sample with 5% Ba up to 25% ca. for the Pt–Ba(23)/γ-Al_2O_3 catalyst sample. Accordingly, it was speculated that the increase in the number of Pt–Ba neighbouring couples that paralleled the increase in the Ba loading favoured the storage of NO_x via the "nitrite route" and thus resulted in a better utilization of the Ba component as well.

Indications on the occurrence of different NO_x adsorption routes, involving either the NO oxidation to NO_2 followed by NO_2 disproportionation, or the direct NO uptake in the presence of oxygen, have also been provided in other literature reports [24,27–30].

SCR – The adsorption of NO_x was also investigated over SCR catalysts, and the interaction of both NO and NO_2 with vanadium-based and Fe-zeolite commercial catalysts was studied performing transient reactive experiments at different temperatures in the range 50–200 °C [99,101].

When NO was fed at 50 °C in the absence of oxygen in the feed to a microreactor loaded either with vanadium or Fe-zeolite system, the measured outlet concentration profile of the reactant was overlapped to the inlet one, an indication of the fact that NO was not significantly stored onto the catalyst surface. The same conclusion was also apparent in the case of experiments run at higher temperatures and/or when also oxygen was present in the feed flow.

A very different picture was observed when studying the adsorption of NO_2. Fig. 3 shows the results collected performing a step addition of 1000 ppm of NO_2 to a feed flow consisting of 1% H_2O and He flowing over a Fe-ZSM5 catalyst at 50 °C [99,101]. At t = 0 s, when NO_2 was admitted to the microreactor, NO evolution was observed, while the outlet concentration of NO_2 exhibited a delay before slowly approaching the feed level. The observed behaviour is in line with the occurrence of NO_2 disproportionation according to reaction (1); indeed, a quantitative analysis of the data reported in Fig. 3 showed that the molar ratio between evolved NO and converted NO_2 was close to 1/3, confirming the stoichiometry of the overall reaction (1).

Accordingly, as in the case of the Lean NO_x Trap chemistry, it is concluded that NO_2 adsorption occurs by a first simultaneous formation of nitrates and nitrites (reaction (1)), followed by the fast oxidation of nitrites to nitrates by NO_2 (reaction (2)), accompanied by NO evolution.

Formation of nitrates at the end of the run was also confirmed by a subsequent TPD run (not shown): heating of the catalyst after NO_2 adsorption resulted in evolution of NO_2, NO and oxygen starting roughly from 200 °C, in line with nitrate decomposition stoichiometry, reaction (5):

$$2NO_3^- \rightarrow 2NO_2 + 1/2O_2 + O^{2-} \quad (5)$$

The capacity to store surface nitrate species via NO_2 disproportion is not peculiar of zeolite systems; indeed similar experiments have been performed over V_2O_5-WO_3/TiO_2 catalysts [96] and similar results have been obtained.

The NO_2 disproportionation reaction over different SCR catalysts is also reported in several papers in the literature [74,75,79,83–87]. Sachtler's group used FTIR spectroscopy to clarify the nature of the surface species involved in the SCR chemistry over different zeolite-based catalysts [68,69,76,79,86]. Accordingly, Yeom et al. [76] showed the simultaneous formation of NO_3^- and NO^+ upon exposure of a BaNa/Y zeolite to NO_2 at 200 °C under dry conditions, via dissociative chemisorption of N_2O_4. It was also shown that NO^+ rapidly reacts with water to form HONO and H^+, hence acting as a nitrites precursor.

Similar results were presented by Rivallan et al. [92]: IR spectra recorded upon NO_2 adsorption at RT over an Fe-ZSM-5 catalyst in the absence of water showed the presence of intense bands associated with NO^+ and NO_3^- species formed onto Fe sites. Also, indirect evidence for the formation of nitrite groups was provided.

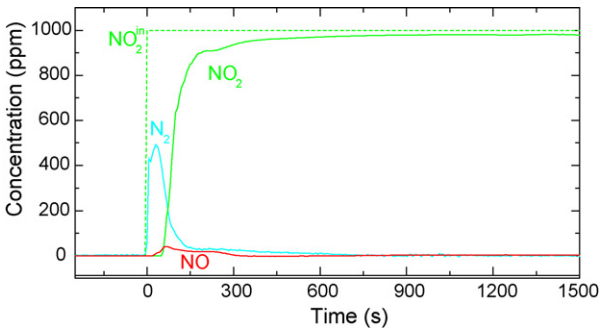

Fig. 4. NO_2 feed at 200 °C over Fe-zeolite catalyst presaturated with ammonia. Feed flow = 71 cm^3/min (STP), NO_2 = 1000 ppm, H_2O = 1% (v/v) in He, after preadsorbing NH_3 (1000 ppm) at 200 °C.

Finally, Iwasaki et al. [88] performed NO_2 adsorption experiments at 100 °C over Fe- and H-ZSM-5 systems and confirmed formation of NO^+ and nitrate ions primarily onto oxo-Fe^{3+} sites. Such aspects have recently been reviewed by Brandenberger et al. [87].

3.2. NO_x reduction processes

The data presented above indicate that in the case of LNT catalysts, nitrites and nitrates are formed during the lean phase upon interaction with NO and/or NO_2. These species are then reduced in the subsequent rich phase during which the stored NO_x are ideally transformed into dinitrogen.

Conversely, in the NH_3-SCR process NO_x species are continuously reduced by ammonia injected in the system. Nevertheless, also in this case significant amounts of NO_x are stored on the catalyst surface whenever the NO_2 concentration in the exhaust entering the SCR reactor is significant, e.g. due to the presence of an oxidation catalyst (DOC unit) positioned upstream of the SCR converter. In fact, it was clearly shown that NO_2 rapidly disproportionates over commercial SCR catalysts to form surface nitrites and nitrates. As shown below, such adsorbed species play a major role in the NO_2-related SCR chemistry.

Accordingly, an extensive investigation has been undertaken in our labs in order to analyze the interaction of NO_x adsorbed species with the reducing agents involved in the two processes, namely ammonia and NO in the case of the SCR process, and hydrogen in the case of LNT catalysts.

SCR – The interaction between ammonia and surface nitrites and nitrates formed by NO_2 disproportionation, was first analyzed.

Experiments feeding 1000 ppm of NO_2 over a catalyst presaturated with ammonia were performed at different temperatures in the range 50–200 °C over an Fe-ZSM5 catalyst. At 50 °C (results not shown) NO_2 was immediately consumed with simultaneous production of NO. Quantitative analysis of the outlet concentration profiles indicate the occurrence of reaction (1) in which NO_2 disproportionates eventually leading to formation of surface nitrates and evolution of NO, as indeed already observed in the absence of ammonia (Fig. 3). Thus, at such low *T*, the disproportionation of NO_2 was essentially unaffected by the presence of adsorbed ammonia on the catalyst surface.

Conversely, at temperatures higher than 100 °C a different situation occurred. Fig. 4 shows the results collected over the Fe-zeolite catalyst by feeding 1000 ppm of NO_2 at 150 °C onto a catalyst sample previously saturated with NH_3 at 150 °C. Upon NO_2 addition to the reactor feed (t = 0 s), evolution of about 500 ppm N_2 was immediately observed while NO_2 was completely consumed. After roughly 70 s the nitrogen concentration decreased and the NO_2 concentration increased approaching the feed value. Integral calculations showed that the molar amount of produced N_2 was equal to that of NH_3 previously stored onto the catalyst. A very similar result was also found at 200 °C (not shown).

The formation of nitrogen instead of NO (observed when NO_2 was fed to the reactor in the absence of preadsorbed ammonia, Fig. 3), is ascribed to the occurrence of reaction (6):

$$NH_4^+ + NO_2^- \leftrightarrow [NH_4NO_2] \rightarrow N_2 + 2H_2O \quad (6)$$

in which ammonia surface species react with nitrites to form nitrogen via formation/decomposition of unstable ammonium nitrite. Thus, in both the experiments shown in Figs. 3 and 4, upon NO_2 addition this species disproportionates leading to the formation of nitrates and nitrites onto the catalyst (reaction (2)): then, while in the absence of ammonia nitrites are oxidized to nitrates by NO_2 (reaction (3)), in the presence of ammonia and at sufficiently high temperature nitrites react with ammonia to form ammonium nitrite which eventually decomposes to N_2 (reaction (6)).

So the reaction between ammonia and nitrites can be faster than that of nitrites with NO_2, and such a reaction leads very selectively to dinitrogen already at low temperature [99,101].

However, it is very well known in the literature [67,84,76] that also nitrates interact with ammonia. Accordingly the reactivity of ammonia towards nitrates was also studied by means of a temperature programmed ramp (TPSR) experiment (from 50 up to 550 °C) in which gaseous NH_3 (1000 ppm) + H_2O (1%, v/v) in He was fed to the reactor after NO_2 adsorption at low temperature (50 °C), i.e. in the presence of nitrates formed by NO_2 disproportionation. Fig. 5A shows the profiles of ammonia, nitrogen, NO, NO_2 and N_2O measured during the T-ramp. Upon heating, after an initial strong NH_3 desorption, ammonia began to be converted around 200 °C, with a conversion peak at about 280 °C. At T > 350 °C the NH_3 consumption began to grow slowly again.

At the same temperatures peaks associated with the formation of N_2O first and then N_2 were observed. The evolution of N_2O started from 200 to 210 °C and reached a maximum near 260–270 °C, while N_2 formation started at 220–230 °C and reached a maximum at 280–290 °C: at higher temperature the N_2 production again increased slowly, mirroring the NH_3 evolution.

Accordingly, the observed conversion of gaseous NH_3 by reaction with surface nitrates leads to two distinct products: N_2O, detected at lower temperature, and nitrogen, measured only slightly above 220 °C. In agreement with literature indications, N_2O is attributed to the thermal decomposition of ammonium nitrate or of its surface precursors, according to reaction (7):

$$NH_4NO_3 \rightarrow N_2O + 2H_2O \quad (7)$$

Indeed, surface nitrates, formed onto the catalyst in the first part of the experiment, react with ammonia at 50 °C to form ammonium nitrate species:

$$NO_3^- + NH_4^+ \leftrightarrow NH_4NO_3 \quad (8)$$

which thermally decompose to N_2O above 180–190 °C according to reaction (7).

In contrast, the N_2 production observed in Fig. 5A can be explained by a direct reaction between nitrates and NH_3, according to the following global stoichiometry:

$$5NH_3 + 3HNO_3 \rightarrow 4N_2 + 9H_2O \quad (9)$$

that occurs at higher temperatures and in principle may involve the intermediate reduction of nitrates to nitrites, followed by formation/decomposition of ammonium nitrite to nitrogen.

Dedicated experiments performed in our labs over the Fe-zeolite catalyst showed that reaction (9) is rate determining in the so-called NO_2-SCR reaction:

$$6NO_2 + 8NH_3 \rightarrow 7N_2 + 12H_2O \quad (10)$$

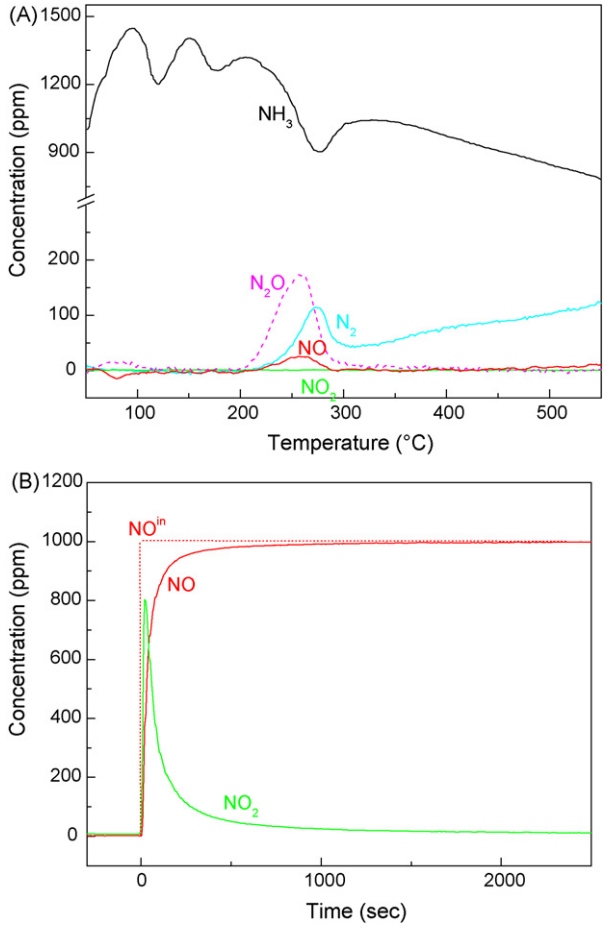

Fig. 5. (A) TPSR experiment of gaseous NH_3 and presaturated with nitrate species over Fe-zeolite catalyst. Feed flow = 71 cm^3/min (STP), NH_3 = 1000 ppm, H_2O = 1% (v/v) in He, T-ramp = 20 °C/min after preadsorbing NO_2 (1000 ppm) at 50 °C (adapted from [101]). (B) NO feed at 50 °C over a catalyst presaturated with nitrates. Feed flow = 71 cm^3/min (STP), NO = 1000 ppm, H_2O = 1% (v/v) in He preadsorbing NO_2 (1000 ppm) at 50 °C (adapted from [102]).

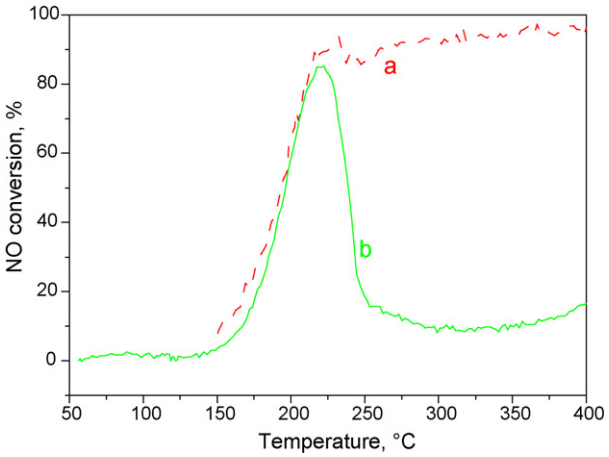

Fig. 6. TPR experiments over Fe-ZSM5. W_{cat} = 0.080 mg, flow rate = 72 cm^3/min (STP). Curve a (Fast SCR): feed = 1% H_2O, 0% O_2, NH_3 = 1000 ppm, NO = 500 ppm, NO_2 = 500 ppm + He. Curve b: feed = 1% H_2O, 0% O_2, NH_3 = 1000 ppm, NO = 1000 ppm + He over catalyst pre-treated with NO_2 (1000 ppm) + H_2O (1%) at 60 °C (adapted from [100]).

that typically occurs on SCR catalysts above 230 °C and in the presence of excess NO_2 ($NO_2/NO_x > 0.5$) [102]. In fact, it has been shown that the "NO_2-SCR" reactivity results from a reaction sequence involving the formation of nitrates from NO_2 disproportionation and their selective reduction by NH_3.

Thus, nitrates are reduced by ammonia: at low temperature via the formation of ammonium nitrate strongly interacting species [102] which can then lead to formation of undesired N_2O, and at higher temperatures to nitrogen (reaction (9)). The comparison with similar data collected on a H-zeolite also showed that the latter reaction (reaction (9)) is catalysed by a redox component: accordingly, a redox interpretation of the catalytic reduction of nitrates by ammonia, wherein NH_3 reduces the catalyst sites which are then reoxidized by surface nitrates with possible intermediate formation of nitrites, was recently proposed [102].

However, NH_3 is not the only potential reducing agent included in the exhaust gases entering the SCR converter: the interaction of surface nitrates with NO has also been investigated. For this purpose 1000 ppm of NO_2 were preliminarily fed at 50 °C to the Fe-zeolite catalyst in the presence of H_2O (1%, v/v) to form and store nitrates onto the catalyst surface (experiment not shown); then, after NO_2 shut off and keeping the temperature constant, 1000 ppm of NO was added to the reactor feed stream in order to study the reactivity of nitric oxide with surface nitrates.

It appears (Fig. 5B) that NO was immediately converted while roughly 800 ppm of NO_2 was formed. Quantitative analysis of the results indicated the occurrence of the reverse of reaction (1), i.e. reaction (1a)

$$2NO_3^- + NO \leftrightarrow 3NO_2 + O^{2-} \quad (1a)$$

Thus, nitrates present on the catalyst surface react with NO producing NO_2 and nitrites according to the reverse of reaction (3), i.e. reaction (3a), and then part of such nitrites are further oxidized by other nitrates according to reverse of reaction (2), reaction (2a):

$$NO_3^- + NO \leftrightarrow NO_2 + NO_2^- \quad (3a)$$

$$NO_3^- + NO_2^- \rightarrow 2NO_2 + O^{2-} \quad (2a)$$

Accordingly, it appears that nitrates are not only reduced by ammonia, but also by gaseous NO; indeed, NO was found very active in reducing surface nitrates already at temperatures as low as 50 °C, even if unable to deplete all of the NO_x stored on the catalyst surface.

To analyze the role of reaction (3a) in the global SCR chemistry we performed a number of dedicated transient reactive experiments [96,98] over both vanadium-based and Fe-zeolite catalysts. Fig. 6 compares the NO conversion profile measured as a function of temperature in TPR runs while feeding: (i) 1000 ppm ammonia and 500 ppm each of NO and NO_2 (curve a), and (ii) equimolar amounts of ammonia (1000 ppm) and NO (but no NO_2) over a catalyst sample presaturated with nitrates (curve b). Results clearly shows that at low temperature curves a and b are superimposed, indicating that the reactivity of NO and ammonia with surface nitrates is equivalent to that of the Fast SCR reaction (11),

$$2NH_3 + NO_2 + NO \rightarrow 2N_2 + 3H_2O \quad (11)$$

that is the most important reaction occurring in the NH_3-SCR system when NO_2 is present in the feed flow due to its very high rates at low temperatures [1,70]. The same conclusion was also derived from transient experiments at constant temperature (170–190 °C) [93,97,99]: the NO conversion levels measured either during the Fast SCR reaction (with NH_3/NO-NO_2) or during the reaction between NH_3/NO and surface nitrates were practically identical, indicating that the two reactions were actually progressing at the same rate. Accordingly, it was proposed that the rate determining step of the *Fast SCR* reaction (11) is the reduction of surface nitrates by NO to nitrites, which then easily reacts with ammonia producing dinitrogen via ammonium nitrite decomposition.

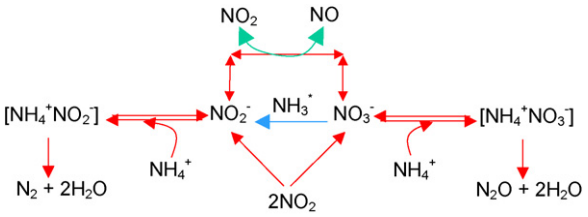

Fig. 7. Reaction pathway for NO-NO_2/NH_3-SCR reactions over V_2O_5-WO_3/TiO_2, Fe-zeolite and Cu-zeolite catalysts.

Fig. 7 shows a schematic summary of the Fast SCR and of the NO_2-SCR chemistry in terms of surface species, which applies to both V_2O_5-WO_3/TiO_2 and Fe-zeolite catalysts. In line with the results discussed above, NO_2 is responsible for the formation of nitrate and nitrite ad-species onto the catalyst surface via disproportion and heterolytic chemisorption (reactions (1–3); nitrites easily react with NH_3 to give dinitrogen and H_2O via decomposition of the unstable ammonium nitrite (reaction (6)); but also nitrates are reduced, at lower temperature (T > 150 °C) by NO, that converts them to nitrites (reaction (3a)), and at higher temperatures (T > 220 °C) by NH_3, that converts them to nitrites or directly to nitrogen (reaction (9)).

Concerning the key role of surface nitrites and nitrates in the NO_2-related SCR chemistry, Weitz et al. [76], on the basis of both spectroscopic evidence and steady-state reaction data, proposed a Fast SCR pathway over a BaNa-Y zeolite which is in close agreement with the one displayed in Fig. 7. A similar picture was also presented by Kröcher and coworkers [84,85]; indeed, based on the analysis of their own data and of literature data, they proposed a common Fast SCR reaction mechanism for transition-metal zeolites and for vanadium-based catalysts.

LNT – Dedicated transient experiments were performed under nearly isothermal conditions where mainly nitrate species were formed and stored at 350 °C over the Pt–Ba/γ-Al_2O_3 catalyst by NO/O_2 adsorption, and then reduced at constant temperature or upon heating using different reducing agents [60,61,64].

Fig. 8A shows the concentration profiles of hydrogen, ammonia and nitrogen versus temperature measured during a TPSR experiment carried out by feeding 2000 ppm of H_2 in the presence of 1% H_2O after having stored NO_x species at 350 °C. Fig. 8A shows that H_2 was consumed starting from roughly 50 °C and a minimum in the H_2 concentration was seen near 100 °C. A very large NH_3 production was detected from low temperature, followed by small amounts of N_2. The stored nitrates were completely reduced at temperatures below 200 °C.

The reactivity of nitrates with hydrogen was also investigated under isothermal conditions at different temperatures, in the range 100–350 °C (Fig. 9). In order to decouple the effects related to the temperature of adsorption of NO_x from that of the temperature of their reduction, in all cases NO_x were adsorbed at 350 °C while the reduction of the stored NO_x was accomplished at different temperatures, in the range 100–350 °C.

The results, shown in Fig. 9, demonstrated that when the reduction of the NO_x stored at 350 °C is carried out at low temperatures (150 and 200 °C), NH_3 is the major reaction product. Upon increasing the reduction temperature, formation of N_2 increases at the expense of ammonia. This leads to a strong increase with temperature of the selectivity to N_2 of the reduction process, from 10% at 100 to near 90% above 250 °C [64]. Notably, during these experiments the evolution of nitrogen at the reactor outlet always precedes that of undesired ammonia.

Similar results were obtained when the NO_x storage and reduction processes were carried out at the same temperatures [59].

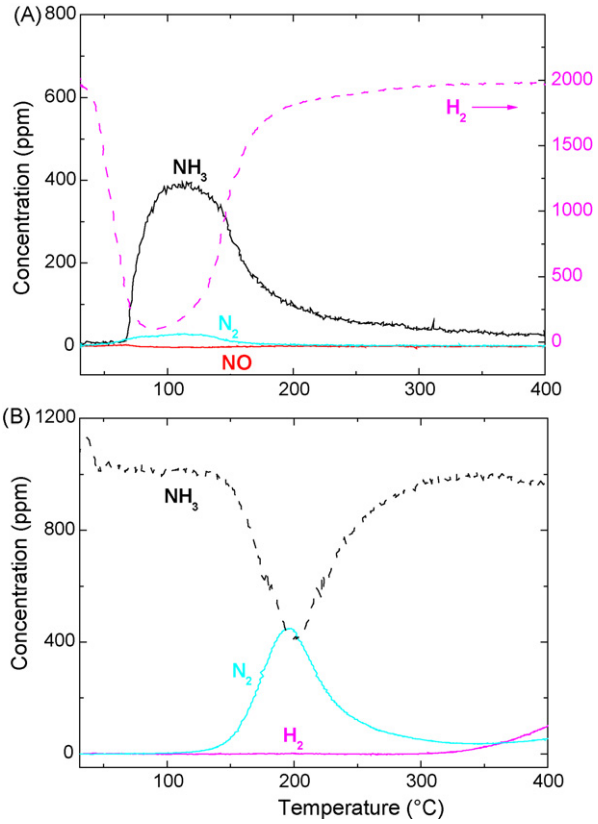

Fig. 8. (A) H_2-TPSR (2000 ppm + 1%, v/v H_2O in He), (B) NH_3-TPSR (1000 ppm + 1%, v/v H_2O in He) after NO/O_2 adsorption at 350 °C over Pt–Ba/γ-Al_2O_3 catalyst (adapted from [64]).

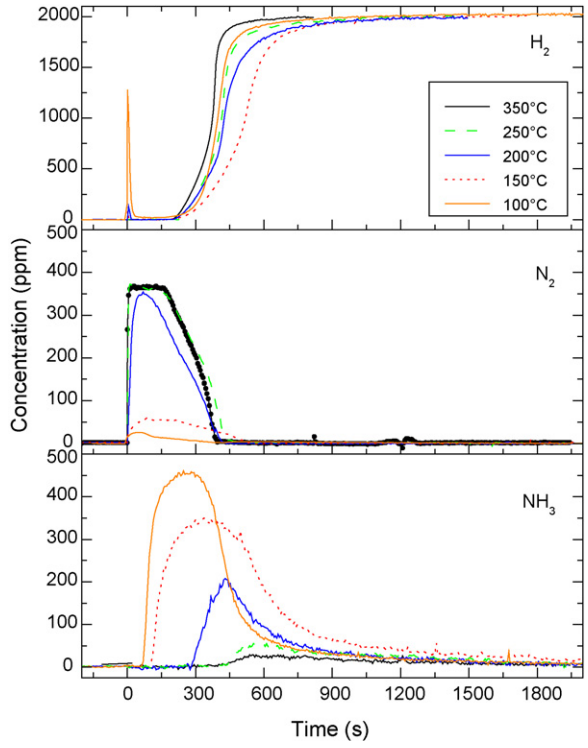

Fig. 9. H_2-ISC experiments (2000 ppm + 1%, v/v H_2O in He) after NO/O_2 adsorption at 350 °C over the Pt–Ba/γ-Al_2O_3 catalyst (adapted from [64]).

The following stoichiometries were identified for the reduction of nitrates by hydrogen leading to nitrogen or ammonia, respectively:

$$Ba(NO_3)_2 + 5H_2 \rightarrow BaO + N_2 + 5H_2O \quad (12)$$

$$Ba(NO_3)_2 + 8H_2 \rightarrow BaO + 2NH_3 + 5H_2O \quad (13)$$

In order to get additional information on the reaction pathway operating during the reduction of the stored nitrates and on the role of ammonia in the reaction, the reactivity of ammonia with adsorbed NO_x was investigated as well. Fig. 8B shows the results of NH_3-TPSR experiments performed feeding 1000 ppm of ammonia in the presence of 1% H_2O over the Pt–Ba/γ-Al_2O_3 catalyst, after having stored NO_x species at 350 °C.

It appears that ammonia was consumed starting from roughly 130 °C with simultaneous formation of nitrogen, according to the following overall stoichiometry:

$$3Ba(NO_3)_2 + 10NH_3 \rightarrow 8N_2 + 3BaO + 15H_2O \quad (14)$$

At temperatures higher than 350 °C the NH_3 concentration decreased again and N_2 and H_2 evolution was observed, due to the occurrence of the ammonia decomposition reaction:

$$2NH_3 \rightarrow N_2 + 3H_2 \quad (15)$$

Accordingly, also in the case of LNT catalyst ammonia is active in the reduction of the stored nitrates: the reaction takes place at relatively low temperatures and leads very selectively to nitrogen.

It is useful to note that reaction (14) is virtually the same as reaction (9), occurring in the SCR process when nitrate species, formed by NO_2 disproportionation, were directly reduced by ammonia to dinitrogen. However, in contrast to that observed in the case of the SCR process, N_2O was never produced in significant amounts when reducing nitrates stored over the LNT catalyst by ammonia. This can be explained on the basis of the different stability of the stored nitrates: in the case of the LNT catalyst, the Ba component stabilizes the nitrates and this prevents the formation of strongly interacting NH_4^+–NO_3^- species whose decomposition has been invoked in the formation of N_2O [101].

Accordingly nitrates stored onto a Ba-based LNT catalyst were easily reduced by H_2 at very low temperatures with formation of ammonia only (Fig. 8A), and ammonia was active in the reduction of the stored nitrates (Fig. 8B) with a complete selectivity to nitrogen but at higher temperatures if compared to H_2 (T_{onset} near 130–140 °C versus 60 °C). This suggests that the formation of N_2 during the regeneration of LNTs by H_2 occurs via an in series 2-step pathway involving at first the fast formation of ammonia upon reaction of nitrates with H_2 (reaction (13)), followed by the slower reaction of ammonia with the stored nitrates leading to the selective formation of N_2 (reaction (14)) [64]. The sum of reactions (13) and (14) leads to the overall stoichiometry for the reduction of nitrates to N_2, reaction (12).

The occurrence of a fast reaction of the adsorbed nitrates with H_2 to give ammonia together with the integral "plug-flow" nature of the reactor imply the complete consumption of the reductant H_2 and the formation of an H_2 front travelling along the reactor axis, which also explains the temporal evolution of the products (with NH_3 evolution following that of N_2, see Fig. 9). As sketched in Fig. 10 where the ongoing reduction process in the catalyst bed is shown, at a given instant of the regeneration phase, different zones are present in the reactor: (i) an initial zone upstream the H_2 front, where the trap has already been regenerated upon reduction of nitrates by H_2; (ii) the zone corresponding to the development of the H_2 front, where the concentration of hydrogen decreases from the inlet value to almost zero and where ammonia formation is occurring (reaction (13)); (iii) a zone immediately downstream the H_2 front where nitrates are still present and, if the temperature is high enough, react with ammonia originated upstream; (iv) a last zone where nitrates initially stored have not yet been involved in any reduction process. When the regeneration of the trap is carried out at low temperatures, e.g. 150 °C or below, H_2 reacts with surface nitrates to give NH_3 according to reaction (13); however, ammonia at such low temperatures can hardly react with the stored nitrates to form N_2 according to reaction (12). As a result ammonia is by far the major reaction product and the nitrogen selectivity is very low. Upon increasing the reduction temperature, the reactivity of NH_3 with nitrates (reaction (14)) becomes appreciable and this leads to the formation of N_2 which is accordingly detected at the reactor outlet. Since H_2 is by far more reactive than NH_3 towards surface nitrates, NH_3 reacts preferentially with nitrates located downstream the H_2 front.

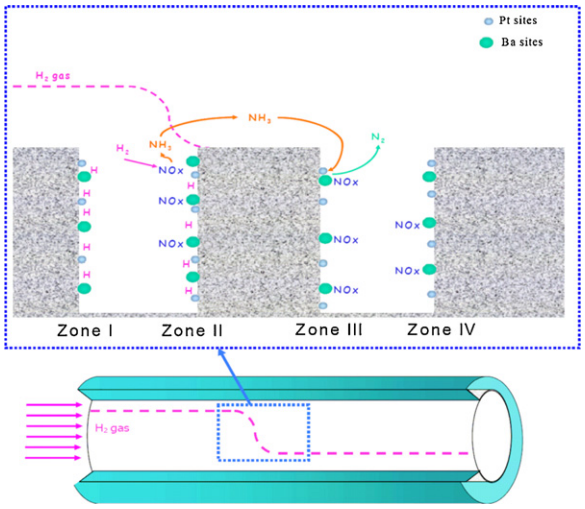

Fig. 10. Sketch of the reduction mechanism for a Pt–Ba/γ-Al_2O_3 catalyst upon regeneration with H_2 (adapted from [64]).

Once the H_2 front reaches the end of the catalyst bed, no nitrates are stored downstream and hence formed ammonia exits the reactor unconverted: accordingly N_2 evolution at the reactor outlet precedes that of NH_3 (Fig. 9).

Also useful to note is that according to this picture, ammonia is an intermediate in N_2 formation and the NH_3 + nitrate reaction is the only route explaining the formation of dinitrogen. However this conclusion has been derived upon analysis of experiments carried out under nearly isothermal conditions, i.e. in the absence of significant temperature effects in the catalyst bed due to the diluted conditions employed and to the presence of a He purge between the lean and the rich switches. Under actual conditions, where significant thermal effects and NO evolutions are occurring during the lean/rich switches, different mechanisms may operate.

A similar pathway has been suggested by Cumaranatunge et al. [57] and by Pihl et al. [52] who proposed that during the regeneration stage a regeneration front travels along the catalyst bed: ammonia and N_2 can be simultaneously formed in the H_2-rich zone of the front, but NH_3 may further react with the stored nitrates leading to the formation of N_2. This would explain the temporal sequence of the products formation with NH_3 breakthrough observed after N_2 production when the stored NO_x starts to deplete and is insufficient to react with the NH_3 formed upstream. However, in these suggested pathways N_2 formation does not uniquely originate upon reaction of NH_3 with surface nitrates. Along these lines, on the basis of in situ FTIR spectroscopy coupled with mass spectrometry and time-resolved XRD, Szailer et al. [54] proposed that the selectivity to $N_2/NH_3/N_2O$ formation depends on the surface concentration of adsorbed Pt. . .N_a, Pt. . .H_a, etc. species. On the other hand, Dhainaut et al. [58] proposed for N_2 formation over sup-

ported Pd catalysts an NH_3-SCR-like mechanism involving NO and adsorbed NH_x fragments, while Kondratenko and Baerns [55] suggested that N_2 formation over Pt supported catalysts could derive both from reaction between NO and NH_x adsorbed species, and from recombination of –N ad-atoms deriving from NO dissociation or NH_3 complete dehydrogenation.

According to the pathway we propose, which involves NH_3 as an intermediate species, the stored NO_x is over-reduced to NH_3 which in turn is required for N_2 formation. Since this pathway has been derived in the case of H_2 as reducing agent, the reduction of NO_x species adsorbed at 350 °C over the alumina supported Pt–Ba catalyst was also investigated using CO as reducing agent. Transient experiments were performed both under temperature programming and under isothermal conditions feeding 2000 ppm of CO in the presence and in the absence of water [66].

The results collected in the absence of water (not reported) showed that CO was able to reduce NO_x adsorbed species producing nitrogen, but at temperatures higher than those measured in the case of hydrogen. Furthermore, data showed that significant amounts of N- and C-containing species were still left onto the catalyst at the end of the reduction process. FTIR spectra identified such species as $^{-}N{=}C{=}O$ (isocyanates) and/or $N{\equiv}C{-}O^{-}$ (cyanates), along with carbonates [66]. Accordingly, the reduction of surface nitrates by CO was described by the following overall stoichiometries,

$$Ba(NO_3)_2 + 8CO \rightarrow Ba(NCO)_2 + 6CO_2 \quad (16)$$

$$Ba(NO_3)_2 + 5CO \rightarrow BaCO_3 + N_2 + 4CO_2 \quad (17)$$

accounting for the formation of cyanates and nitrogen, respectively, along with carbonates. It is useful to note that almost complete reduction of the initially stored NO_x was obtained with CO, although N_2 evolution was much less than the amounts of the stored NO_x. In fact significant amounts of reduced NO_x species are left adsorbed on the catalyst surface in the form of isocyanate and cyanate ad-species; interestingly, these species are characterized by a formal oxidation state of the N atom equal to −3, like ammonia.

It has been suggested that NCO^{-} ad-species are not spectator or terminal species, but are in fact intermediates in the formation of nitrogen [66]. It is indeed well known that NCO species are easily oxidized to N_2 and CO_2 by oxidant molecules like O_2 [43]; in line with previous suggestions reported by Szailer et al. [54], a pathway for N_2 formation involving the oxidation of cyanates by other oxidants like surface NO_x species (e.g unreacted nitrate species adsorbed close-by to the cyanate/isocyanate species) can be envisaged, this step being rate determining in N_2 formation.

The same experiments were performed in the presence of water in the feed flow: it was found that water enhanced the reactivity of CO and higher NO_x removal efficiencies were achieved as compared to dry conditions. Besides, significant amounts of ammonia and hydrogen were found among the products, together with nitrogen and CO_2. It is useful to note that FTIR spectra did not evidence any significant presence of NCO species.

A possible explanation is that cyanate/isocyanate species form even in the presence of water, but are readily hydrolyzed to ammonia and CO_2. This would also explain the presence of ammonia among the reaction products [66]. Alternatively, it may be speculated that in the presence of water the reduction of nitrates may involve H_2 as reducing agent, formed according to the WGS reaction that is active over LNT catalysts in the same temperature range.

Accordingly, under wet conditions different pathways likely operate during the reduction of nitrates by CO: a first pathway involves cyanate/isocyanates formation, which are then readily hydrolyzed to ammonia. As shown in the case of H_2 as reductant, ammonia is then involved in the reduction of nitrates to N_2. A second route involves the formation of hydrogen from CO and water via the water gas shift reaction: the so formed H_2 then reacts with nitrates to form ammonia according to the lines depicted above in the case of H_2.

Thus, the data converge in indicating that both when H_2 and CO are used as reducing agent, ammonia (or an N-containing species with the N atom in the -3 formal oxidation state) is intermediate in the formation of N_2. This species is hence originated by reaction with adsorbed NO_x through a pathway which is presently under investigation in our labs.

4. Conclusions

In this work mechanistic aspects of the reduction of NO_x according to both LNT and SCR techniques have been considered. These technologies are considered alternatives for the removal of NO_x from the exhausts of lean combustion engines: however a detailed investigation of the pathways effecting the NO_x reduction in these two different processes has pointed out several analogies (along with some differences).

In the case of the LNT systems, which operate under cyclic conditions, NO_x is stored in the form of nitrates and nitrites during a long lean phase and then reduced to N_2 and other byproducts (e.g. NH_3) during a short rich period. Under near isothermal conditions, it was found that when H_2 or CO are employed as reducing agents, the reduction process is not initiated by the thermal decomposition of the stored NO_x ad-species, but rather by a catalytic pathway involving Pt. In the case of H_2, such a catalytic pathway is composed of two consecutive steps in which the reaction of nitrates with H_2 leads to the formation of intermediate NH_3, which further reacts with nitrates to produce selectively N_2. Ammonia (or cyanate/isocyanate adsorbed species) act as intermediate species in N_2 formation when the reduction is carried out with CO instead of H_2 as reducing agents.

In contrast to LNTs, the SCR technology does not operate under cyclic conditions, but the reduction of the NO_x is achieved by continuous NH_3 injection in the exhaust gases prior to the SCR converter. However, the analysis of the NH_3-NO/NO_2-SCR reacting system by an extensive set of unsteady experiments performed over both vanadium-based and zeolite-based commercial catalysts proved that NO_x adsorbed species (nitrates and nitrites) play a key role in the SCR chemistry as well. In particular, it was found that nitrate species are formed on the catalyst surface by NO_2 disproportion and are reduced by either NO or NH_3 to nitrites: such species eventually and selectively lead to nitrogen upon further reaction with ammonia.

Thus, in both LNT and SCR techniques, the reduction of NO_x involves the formation of nitrite and nitrate surface species, which are eventually reduced to nitrogen by ammonia, either formed as an intermediate (LNT) or supplied as a reactant (SCR).

Acknowledgments

DAIMLER AG is gratefully acknowledged for financial support of the SCR project.

MIUR (Roma) is gratefully acknowledged for financial support of the LNT project.

References

[1] T. Johnson, Platinum Met. Rev. 52 (2008) 23.
[2] Association for Emissions Control by Catalyst Website, www.aecc.eu.
[3] W.S. Epling, L.E. Campbell, A. Yezerets, N.W. Currier, J.E. Park II, Catal. Rev. Sci. Eng. 46 (2004) 163.
[4] R. Burch, Catal. Rev. Sci. Eng. 46 (2004) 271.
[5] E. Fridell, M. Skoglundh, B. Westerberg, S. Johansson, G. Smedler, J. Catal. 183 (1999) 196.
[6] H. Mahzoul, J.F. Brilhac, P. Gilot, Appl. Catal. B: Environ. 20 (1999) 47.
[7] E. Fridell, H. Persson, B. Westerberg, L. Olsson, M. Skoglundh, Catal. Lett. 66 (2000) 71.

[8] T. Maunula, J. Ahola, H. Hamada, Appl. Catal. B: Environ. 26 (2000) 173.
[9] B. Westerberg, E. Fridell, J. Mol. Catal. A: Chem. 165 (2001) 249.
[10] L. Olsson, H. Persson, E. Fridell, M. Skoglundh, B. Andresson, J. Phys. Chem. B 105 (2001) 6895.
[11] H.Y. Huang, R.Q. Long, R.T. Yang, Energy & Fuels 15 (2001) 205.
[12] P.J. Schmitz, R.J. Baird, J. Phys. Chem. B 106 (2002) 4172.
[13] N.V. Cant, M.J. Patterson, Catal. Today 73 (2002) 271.
[14] P. Broqvist, I. Panas, E. Fridell, H. Persson, J. Phys. Chem. B 106 (2002) 137.
[15] C. Hess, J.H. Lunsford, J. Phys. Chem. B 106 (2002) 6358.
[16] C. Hess, J.H. Lunsford, J. Phys. Chem. B 107 (2003) 1982.
[17] F. Laurent, C.J. Pope, H. Mahzoul, L. Delfosse, P. Gilot, Chem. Eng. Sci. 58 (2003) 1793.
[18] P.T. Fanson, M.R. Horton, W.N. Delgass, J. Lauterbach, Appl. Catal. B: Environ. 46 (2003) 393.
[19] J.A. Anderson, B. Bachiller-Baeza, M. Fernández-García, Phys. Chem. Chem. Phys. 5 (2003) 4418.
[20] D. James, E. Fourre, M. Ishii, M. Bowker, Appl. Catal. B: Environ. 45 (2003) 147.
[21] W.S. Epling, G.C. Campbell, J.E. Parks, Catal. Lett. 90 (2003) 45.
[22] M. Piacentini, M. Maciejewski, T. Bürgi, A. Baiker, Top. Catal. 30/31 (2004) 71.
[23] P. Svedberg, E. Jobson, S. Erkfeldt, B. Andersson, M. Larsson, M. Skoglund, Top. Catal. 30/31 (2004) 199.
[24] U. Tuttlies, V. Schmeißer, G. Eigenberger, Chem. Eng. Sci. 59 (2004) 4731.
[25] J. Szanyi, J.H. Kwak, J. Hanson, C. Wang, T. Szailer, C.H.F. Peden, J. Phys. Chem. B 109 (2005) 7339.
[26] D.H. Kim, Y.H. Chin, J.H. Kwak, J. Szanyi, C.H.F. Peden, Catal. Lett. 105 (2005) 259.
[27] K.S. Kabin, P. Khanna, R.L. Muncrief, V. Medhekar, M.P. Harold, Catal. Today 114 (2006) 72.
[28] C.M.L. Scholz, V.R. Gangwal, J.H.B.J. Hoebink, J.C. Schouten, Appl. Catal. B 70 (2007) 226.
[29] J. Szanyi, J.H. Kwak, D.H. Kim, X. Wang, R. Chimentao, J. Hanson, W.S. Epling, C.H.F. Peden, J. Phys. Chem. C 111 (2007) 4678.
[30] J. Szanyi, J.H. Kwak, D.H. Kim, X. Wang, J. Hanson, R. Chimentao, C.H.F. Peden, Chem. Commun. (2007) 984.
[31] M. Bowker, Chem. Soc. Rev. 37 (2008) 2204.
[32] L. Lietti, P. Forzatti, I. Nova, E. Tronconi, J. Catal. 204 (2001) 175.
[33] F. Prinetto, G. Ghiotti, I. Nova, L. Lietti, E. Tronconi, P. Forzatti, J. Phys. Chem. B 105 (2001) 12732–12745.
[34] I. Nova, L. Castoldi, F. Prinetto, G. Ghiotti, L. Lietti, E. Tronconi, P. Forzatti, J. Catal. 222 (2004) 377.
[35] I. Nova, L. Castoldi, F. Prinetto, V. Dal Santo, L. Lietti, E. Tronconi, P. Forzatti, G. Ghiotti, R. Psaro, S. Recchia, Top. Catal. 30/31 (2004) 181.
[36] L. Castoldi, I. Nova, L. Lietti, E. Tronconi, P. Forzatti, Catal. Today 96 (2004) 43.
[37] A. Scotti, I. Nova, E. Tronconi, L. Castoldi, L. Lietti, P. Forzatti, Ind. Eng. Chem. Res. 43 (2004) 4522.
[38] I. Nova, L. Castoldi, L. Lietti, E. Tronconi, P. Forzatti, SAE Technical Paper, 2005-01-1085.
[39] J.M. Coronado, J.A. Anderson, J. Mol. Catal. A: Chem. 138 (1999) 83.
[40] M. Stoica, M. Caldararu, N.I. Ionescu, A. Auroux, Appl. Surf. Sci. 153 (2000) 218.
[41] R. Burch, J.P. Breen, F.C. Meunier, Appl. Catal. B: Environ. 39 (2002) 283.
[42] J.P. Breen, R. Burch, N. Lingaiah, Catal. Lett. 79 (2002) 171.
[43] T. Lesage, C. Terrier, P. Bazin, J. Saussey, M. Daturi, Phys. Chem. Chem. Phys. 5 (2003) 4435.
[44] S. Poulston, R. Rajaram, Catal. Today 81 (2003) 603.
[45] N.W. Cant, M.J. Patterson, Catal. Lett. 85 (2003) 153.
[46] M. Machida, D. Kurogi, T. Kijima, J. Phys. Chem. B 107 (2003) 196.
[47] Z. Liu, J.A. Anderson, J. Catal. 224 (2004) 18.
[48] H. Abdulhamid, E. Fridell, M. Skoglundh, Top. Catal. 30/31 (2004) 161.
[49] K.S. Kabin, R.L. Muncrief, M.P. Harold, Cat. Today 96 (2004) 79.
[50] M. Sharma, M.P. Harold, V. Balakotaiah, Ind. Eng. Chem. Res. 44 (2005) 6264.
[51] T. Szailer, J.H. Kwak, D.H. Kim, J.C. Hanson, C.H.F. Peden, J. Szanyi, J. Catal. 239 (2006) 51.
[52] J.A. Pihl, J.E. Parks II, C.S. Daw, T.W. Root, SAE Technical Paper, 2006-01-3441.
[53] J.R. Theis, H.W. Jen, R.W. McCabe, M. Sharma, V. Balakotaiah, M.P. Harold, SAE Technical Paper, 2006-01-1067.
[54] T. Szailer, J.H. Kwak, D.H. Kim, J. Szanyi, C. Wang, C.H.F. Peden, Catal. Today 114 (2006) 86.
[55] V.A. Kondratenko, M. Baerns, Appl. Catal. B: Environ. 70 (2007) 111.
[56] D.H. Kim, J.H. Kwak, J. Szanyi, S.D. Burton, C.H.F. Peden, Appl. Catal. B: Environ. 72 (2007) 233.
[57] L. Cumaranatunge, S.S. Mulla, A. Yezerets, N.W. Currier, W.N. Delgass, F.H. Ribeiro, J. Catal. 246 (2007) 29.
[58] F. Dhainaut, S. Pietrzyk, P. Granger, Appl. Catal. B: Environ. 70 (2007) 100.
[59] P. Forzatti, L. Lietti, The reduction of NO_x stored on LNT and combined LNT–SCR systems, Catal. Today (2009), doi:10.1016/j.cattod.2008.11.023.
[60] I. Nova, L. Lietti, L. Castoldi, E. Tronconi, P. Forzatti, J. Catal. 239 (2006) 244.
[61] I. Nova, L. Castoldi, L. Lietti, E. Tronconi, P. Forzatti, SAE Technical Paper, 2006-01-1368.
[62] I. Nova, L. Castoldi, L. Lietti, E. Tronconi, P. Forzatti, Top. Catal. 42–43 (2007) 21.
[63] L. Castoldi, I. Nova, L. Lietti, E. Tronconi, P. Forzatti, Top. Catal. 42–43 (2007) 189.
[64] L. Lietti, I. Nova, P. Forzatti, J. Catal. 257 (2008) 270.
[65] I. Nova, L. Lietti, P. Forzatti, Catal. Today 136 (2008) 128.
[66] I. Nova, L. Lietti, P. Forzatti, F. Frola, F. Prinetto, G. Ghiotti, Top. Catal. 52 (2009) 1767.
[67] M. Koebel, M. Elsener, G. Madia, Ind. Eng. Chem. Res. 40 (2001) 52.
[68] Qi Sun, Z. Gao, H. Chen, W.H. Sachtler, J. Catal. 201 (2001) 89.
[69] Qi Sun, Z. Gao, B. Wen, W.H. Sachtler, Catal. Lett. 78 (2002) 1.
[70] M. Koebel, G. Madia, M. Elsener, Catal. Today 73 (2002) 239.
[71] G. Madia, M. Koebel, M. Elsener, A. Wokaun, Ind. Eng. Chem. Res. 41 (2002) 3512.
[72] M. Koebel, G. Madia, F. Raimondi, A. Wokaun, J. Catal. 209 (2002) 159.
[73] M. Wallin, C.J. Karlsson, M. Skoglundh, A. Palmqvist, J. Catal. 218 (2003) 354.
[74] J. Despres, M. Koebel, O. Kröcher, M. Elsener, A. Wokaun, Micropor. Mesopor. Mater. 58 (2003) 175.
[75] G. Li, C.A. Jones, V.H. Grassian, S.C. Larsen, J. Catal. 234 (2005) 401.
[76] Y.H. Yeom, J. Henao, M.J. Li, W.M.H. Sachtler, E. Weitz, J. Catal. 231 (2005) 181.
[77] K. Rahkamaa-Tolonen, T. Maunula, M. Lomma, M. Huuhtanen, R. Keiski, Catal. Today 100 (2005) 217.
[78] M. Schwidder, M.S. Kumar, K. Klementiev, M.M. Pohl, A. Brückner, W. Grünert, J. Catal. 231 (2005) 314.
[79] M. Li, Y. Yeom, E. Weitz, W.M.H. Sachtler, J. Catal. 235 (2005) 201.
[80] G. Delahay, D. Valade, A. Guzma-Vargas, B. Coq, Appl. Catal. B: Environ. 55 (2005) 149.
[81] O. Kröcher, M. Devadas, M. Elsener, A. Wokaun, N. Söger, M. Pfeifer, Y. Demel, L. Mussmann, Appl. Catal. B: Environ. 66 (2006) 208.
[82] H. Sjövall, L. Olsson, E. Fridell, R.J. Blint, Appl. Catal. B: Environ. 64 (2006) 180.
[83] M.S. Kumar, M. Schwidder, W. Grünert, U. Bentrup, A. Brückner, J. Catal. 239 (2006) 173.
[84] M. Devadas, O. Kröcher, M. Elsener, A. Wokaun, N. Söger, M. Pfeifer, Y. Demel, L. Mussmann, Appl. Catal. B: Environ. 67 (2006) 187.
[85] M. Devadas, O. Kröcher, M. Elsener, A. Wokaun, G. Mitrikas, N. Söger, M. Pfeifer, Y. Demel, L. Mussmann, Catal. Today 119 (2007) 137.
[86] A. Savara, M.J. Li, W.M.H. Sachtler, E. Weitz, Appl. Catal. B: Environ. 81 (2008) 251.
[87] S. Brandenberger, O. Kroecher, A. Tissler, R. Althoff, Catal. Rev. Sci. Eng. 50 (2008) 492.
[88] M. Iwasaki, K. Yamazaki, K. Banno, H. Shinjoh, J. Catal. 260 (2008) 205.
[89] G. Qi, Y. Wang, R.T. Yang, Catal. Lett. 121 (2007) 111.
[90] J. Girard, G. Cavataio, R. Snow, C. Lambert, SAE Technical Paper, 2008-01-1185.
[91] L. Xu, R. McCabe, W. Ruona, G. Cavataio, SAE Technical Paper, 2009-01-285.
[92] M. Rivallan, G. Ricchiardi, S. Bordiga, A. Zecchina, J. Catal. 264 (2009) 104.
[93] C. Ciardelli, I. Nova, E. Tronconi, D. Chatterjee, B. Bandl-Konrad, Chem. Commun. (2004) 2718.
[94] I. Nova, C. Ciardelli, E. Tronconi, D. Chatterjee, B. Bandl-Konrad, Catal. Today 114 (2006) 3.
[95] C. Ciardelli, I. Nova, E. Tronconi, B. Bandl-Konrad, D. Chatterjee, M. Weibel, B. Krutzsch, Appl. Catal. B: Environ. 70 (2007) 80–90.
[96] E. Tronconi, I. Nova, C. Ciardelli, D. Chatterjee, M. Weibel, J. Catal. 245 (2007) 1.
[97] I. Nova, C. Ciardelli, E. Tronconi, D. Chatterjee, M. Weibel, Top. Catal. 42–43 (2007) 43.
[98] C. Ciardelli, I. Nova, E. Tronconi, M. Ascherfeld, W. Fabinski, Top. Catal. 42–43 (2007) 161.
[99] A. Grossale, I. Nova, E. Tronconi, D. Chatterjee, M. Weibel, J. Catal. 256 (2008) 312.
[100] A. Grossale, I. Nova, E. Tronconi, Catal. Today 136 (2008) 18.
[101] A. Grossale, I. Nova, E. Tronconi, J. Catal. 265 (2009) 141.
[102] A. Grossale, I. Nova, E. Tronconi, Catal. Lett. 130 (2009) 525.
[103] A. Grossale, I. Nova, E. Tronconi, D. Chatterjee, M. Weibel, Top. Catal. 52 (2009) 1837.